



## Microbial turnover of glyphosate to biomass: utilization as nutrient source, formation of AMPA and biogenic NER in an OECD 308 test

Brock, Andreas Libonati; Rein, Arno; Polesel, Fabio; Nowak, Karolina Malgorzata; Kästner, Matthias; Trapp, Stefan

*Published in:*  
Environmental Science and Technology

*Link to article, DOI:*  
[10.1021/acs.est.9b01259](https://doi.org/10.1021/acs.est.9b01259)

*Publication date:*  
2019

*Document Version*  
Peer reviewed version

[Link back to DTU Orbit](#)

*Citation (APA):*  
Brock, A. L., Rein, A., Polesel, F., Nowak, K. M., Kästner, M., & Trapp, S. (2019). Microbial turnover of glyphosate to biomass: utilization as nutrient source, formation of AMPA and biogenic NER in an OECD 308 test. *Environmental Science and Technology*, 53(10), 5838-5847. <https://doi.org/10.1021/acs.est.9b01259>

---

### General rights

Copyright and moral rights for the publications made accessible in the public portal are retained by the authors and/or other copyright owners and it is a condition of accessing publications that users recognise and abide by the legal requirements associated with these rights.

- Users may download and print one copy of any publication from the public portal for the purpose of private study or research.
- You may not further distribute the material or use it for any profit-making activity or commercial gain
- You may freely distribute the URL identifying the publication in the public portal

If you believe that this document breaches copyright please contact us providing details, and we will remove access to the work immediately and investigate your claim.

## Environmental Modeling

**Microbial turnover of glyphosate to biomass: utilization as nutrient source, formation of AMPA and biogenic NER in an OECD 308 test**Andreas Libonati Brock, Arno Rein, Fabio Polesel, Karolina  
Malgorzata Nowak, Matthias Kästner, and Stefan Trapp*Environ. Sci. Technol.*, **Just Accepted Manuscript** • DOI: 10.1021/acs.est.9b01259 • Publication Date (Web): 17 Apr 2019Downloaded from <http://pubs.acs.org> on April 23, 2019**Just Accepted**

“Just Accepted” manuscripts have been peer-reviewed and accepted for publication. They are posted online prior to technical editing, formatting for publication and author proofing. The American Chemical Society provides “Just Accepted” as a service to the research community to expedite the dissemination of scientific material as soon as possible after acceptance. “Just Accepted” manuscripts appear in full in PDF format accompanied by an HTML abstract. “Just Accepted” manuscripts have been fully peer reviewed, but should not be considered the official version of record. They are citable by the Digital Object Identifier (DOI®). “Just Accepted” is an optional service offered to authors. Therefore, the “Just Accepted” Web site may not include all articles that will be published in the journal. After a manuscript is technically edited and formatted, it will be removed from the “Just Accepted” Web site and published as an ASAP article. Note that technical editing may introduce minor changes to the manuscript text and/or graphics which could affect content, and all legal disclaimers and ethical guidelines that apply to the journal pertain. ACS cannot be held responsible for errors or consequences arising from the use of information contained in these “Just Accepted” manuscripts.

1 **Microbial turnover of glyphosate to biomass: utilization as nutrient**  
2 **source, formation of AMPA and biogenic NER in an OECD 308 test**

3 Andreas Libonati Brock<sup>1</sup>, Arno Rein<sup>2</sup>, Fabio Polesel<sup>1</sup>, Karolina M. Nowak<sup>3</sup>, Matthias  
4 Kästner<sup>3\*</sup>, Stefan Trapp<sup>1</sup>

5

6 <sup>1</sup>Department of Environmental Engineering, Technical University of Denmark, Bygningstorvet 115,  
7 2800 Kgs. Lyngby, Denmark

8 <sup>2</sup>Chair of Hydrogeology, Technical University of Munich, Arcisstrasse 21, Munich 80333, Germany

9 <sup>3</sup>Helmholtz-Centre for Environmental Research – UFZ, Department of Environmental  
10 Biotechnology, Permoserstrasse 15, 04318 Leipzig, Germany

11

12 *\*Corresponding author:*

13 *Matthias Kästner, e-mail: matthias.kaestner@ufz.de, phone: +49 341/235-1235; Fax: +49 341/235-*  
14 *451235*

15

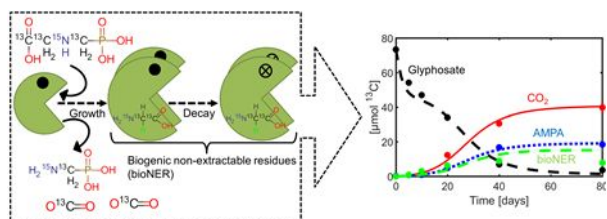
16

17

## 18 TOC Art

19

20



21 **Abstract**

22 Environmental fate assessment of chemicals involves standardized simulation tests with isotope-  
23 labeled molecules to balance transformation, mineralization, and formation of non-extractable  
24 residues (NER). Methods to predict microbial turnover and biogenic NER have been developed,  
25 having limited use when metabolites accumulate, the chemicals are not the only C source, or  
26 provides for other macro-elements. To improve predictive capability, we extended a recently  
27 developed method for microbial growth yield estimation for incomplete degradation and multiple-  
28 element assimilation and combined it with a dynamic model for fate description in soils and  
29 sediments. We evaluated the results against the unique experimental data of  $^{13}\text{C}_3$ - $^{15}\text{N}$ -co-labelled  
30 glyphosate turnover with AMPA formation in water-sediment systems (OECD 308). Balancing  $^{13}\text{C}$ -  
31 and  $^{15}\text{N}$ - fluxes to biomass, showed a pronounced shift of glyphosate transformation from full  
32 mineralization to AMPA formation. This may be explained by various hypotheses, e.g. the limited  
33 substrate turnover inherent to the batch conditions of the test system causing microbial starvation  
34 or inhibition by P release. Modeling results indicate initial N overload due to the lower C/N ratio in  
35 glyphosate compared to average cell composition leading to subsequent C demand and  
36 accumulation of AMPA.

37

38 **Keywords:** bound residues, Gibbs Free Energy, microbial growth yield, non-extractable residues,  
39 simulation, aminomethylphosphonic acid

40

41

42

43

## 44 **1 Introduction**

45 All chemicals sold commercially in the European Union (EU) require approval under the EU  
46 chemicals legislation REACH<sup>1</sup>. Standardized simulation tests (e.g. OECD tests 307<sup>2</sup> and 308<sup>3</sup>)  
47 applying radio- or stable isotope labeled molecules in water, soils, and sediments are used for  
48 gaining sufficient information about the general environmental fate and persistence.<sup>4,5</sup> However,  
49 there is still a debate about interpreting OECD 308 tests combining gas-water-sediment interfaces,  
50 in particular if the deviation of DegT50 (which is the time until 50% of the parent chemical is  
51 degraded) in water and sediments is considered.<sup>3,6–8</sup> In these tests, the turnover is balanced  
52 between mineralization, transformation products and the formation of non-extractable residues  
53 (NER).

54 Particular focus for persistence assessment of a chemical is on the formation of NER, which are  
55 always formed during such simulation tests,<sup>9</sup> and can be the largest fraction (up to 90%) of initial  
56 label mass at the end of a test.<sup>10</sup> NER are determined by the presence of the isotope label after  
57 exhaustive extractions of solid matrices (sediment, soil, sludge, suspended particles etc.) with  
58 limited information about their speciation.<sup>9,11,12</sup> Until recently, neither the potential risk nor the  
59 composition of the NER could be reliably determined.<sup>9</sup> The limited knowledge of the NER  
60 speciation resulted in conflicting conclusions regarding the persistence of the active parent  
61 chemicals.<sup>5,13,14</sup> Previous NER definitions have promoted a mismatch between the legislation and  
62 the state of knowledge in research and modeling. Only parent compounds and primary metabolites  
63 are defined as NER, whereas label conversion to natural bio-components (bioNER), which pose no  
64 risk, is explicitly excluded e.g. in the widely accepted definition of Roberts.<sup>15</sup> However, NER  
65 assessment based on the remaining isotope labels always include bioNER thus resulting in an  
66 overestimation of the potential risks and persistence.<sup>3,6</sup>

67 Recent advances in analytical methods and theories have helped elucidating the nature and  
68 composition of NER and identified bioNER as a major fraction of the formed NER.<sup>9,11,12,16–19</sup> This  
69 has improved the knowledge obtained from OECD tests regarding the potential risks to the  
70 environment and human health.<sup>5</sup> Recently, a method for predicting microbial growth yields of  
71 chemicals (Microbial Turnover to Biomass, MTB) was developed<sup>20</sup> providing the opportunity to  
72 estimate the potential bioNER formation. This method has been applied to estimate bioNER  
73 formed from 40 chemicals of environmental concern<sup>21</sup> and, in addition, to predict input parameters  
74 for use in the 'unified model for biodegradation and sorption'.<sup>20</sup> With the MTB method, the microbial  
75 growth yield can be predicted under the assumption of complete mineralization of the parent  
76 compound with productive growth for various terminal electron acceptors (O<sub>2</sub>, NO<sub>3</sub><sup>-</sup>, SO<sub>4</sub><sup>2-</sup>).  
77 However, metabolites may accumulate diminishing both the matter flux of macro-elements (C, N,  
78 P) and the energy gain of the microorganism, eventually resulting in lower growth yields. To date,

79 the MTB method considered the substrate use as C and energy source for the microorganisms  
80 while certain substrates may also provide other macro-elements (N, P) at defined stoichiometric  
81 ratios. These two factors need to be accounted for in model-based assessment of chemical  
82 persistence.

83 Glyphosate is the most widely applied herbicide worldwide<sup>22</sup> and is subject of public and scientific  
84 debate. Due to its widespread usage, much is known about its fate in the environment for a wide  
85 range of conditions in different matrices.<sup>23–29</sup> Different microorganisms have been isolated capable  
86 of using glyphosate as a source of C, N, and P and energy<sup>24,30–35</sup> but the macro-element relations  
87 have never been thoroughly evaluated. Glyphosate is known to be biodegraded via (at least) two  
88 pathways, namely the so-called sarcosine pathway and the aminomethylphosphonic acid (AMPA)  
89 pathway.<sup>36–39</sup> In the sarcosine pathway, the C-P bond is cleaved via sarcosine (N-methylglycine)  
90 and ortho-phosphate with subsequent complete mineralisation. Sarcosine was never released as  
91 metabolite in these experiments but microbial degradation pathways were commonly agreed to  
92 occur via this intermediate. However, recent abiotic experiments also showed that glyphosate may  
93 directly oxidize in the presence of birnessite to glycine without release of sarcosine.<sup>40</sup>

94 In the AMPA pathway, the C-N bond is cleaved producing AMPA and glyoxylate. AMPA is  
95 considered to be the dominating metabolite that accumulates and is frequently detected in soils  
96 treated with glyphosate and in adjacent surface waters and sediments.<sup>24,41–43</sup> Fortunately, the  
97 environmental fate of <sup>13</sup>C and <sup>15</sup>N co-labeled glyphosate in a water-sediment system (OECD 308)  
98 was studied recently for the first time,<sup>38</sup> and transfer to biomass and bioNER formation was  
99 examined by analysis of the dual label incorporation into amino acids hydrolyzed from microbial  
100 proteins. In parallel to these processes, also AMPA accumulated. This data set provides the  
101 unique opportunity to extend the MTB method combined with the 'unified model for biodegradation  
102 and sorption' to multi-element use and incomplete degradation even in multi-phase systems.

103 Therefore, the aim of the present study was to improve predictive capabilities of environmental fate  
104 models and to capture these phenomena and to exploit the unique <sup>13</sup>C and <sup>15</sup>N co-labeled  
105 glyphosate data for evaluating the developed combined modeling methods for optimized  
106 interpretation of OECD 308 test systems. We aimed at describing metabolite formation (AMPA) as  
107 well as energy gain and macro-element fluxes (C and N) into microbial biomass. In addition, we  
108 derived and evaluated hypotheses about the metabolite formation and shifts of the metabolic  
109 pathways, for example the limitation of microbial growth by other macro-elements than C, here N,  
110 which is not mineralized and may cause N overflow in microbial cells. Substrate consumption,  
111 formation of products and biomolecules, and distribution of labeled C and N were analyzed to  
112 assess metabolic fluxes and macro-element availability.

113

## 114 2 Materials and Methods

115 **Experimental data.** The authors of the co-labelled glyphosate environmental fate study<sup>38</sup> kindly  
 116 provided us with their original experimental data for model evaluation. Briefly the analyses included  
 117 <sup>13</sup>CO<sub>2</sub>, the extractable <sup>13</sup>C and <sup>15</sup>N fractions in water and sediment, non-extractable <sup>13</sup>C and <sup>15</sup>N  
 118 fractions in sediment. Amino acids, hydrolyzed from the parent proteins, and their isotopic  
 119 composition were analyzed in the living microbial biomass fraction of sediment and in the total  
 120 amino acid pool of the sediment fraction (sum of amino acids in both living and dead biomass).  
 121 BioNER were quantified from the amount of <sup>13</sup>C and <sup>15</sup>N in amino acids. Both glyphosate and its  
 122 major metabolite AMPA were measured in water and sediment. A schematic overview of the  
 123 experimental system is shown in Figure S2a (for more details see Wang et al.<sup>38</sup>).

124 **Growth yields.** Theoretical microbial growth yields<sup>20,21</sup> were calculated for glyphosate degradation  
 125 via the sarcosine and the AMPA pathways and served as input to the ‘unified model for  
 126 biodegradation and sorption’.<sup>20</sup> The yield, *Y*, defined as the biomass formed per mass of chemical  
 127 consumed, was determined from the Gibbs free energy of the transformation reaction combined  
 128 with knowledge of the chemical’s structure and microbial growth processes.<sup>20</sup>

129 When the mineralization of a chemical requires many steps or is carried out by a multitude of  
 130 bacterial strains, the assumption of single-step mineralization may no longer be valid.<sup>44</sup> The  
 131 determination of partial growth yields requires the description of individual metabolic steps and the  
 132 flux of macro-elements, energy and electrons within the system must be considered.<sup>44</sup> The MTB  
 133 method can accommodate stepwise transformation by adapting two parameters, namely the  
 134 number of electrons, *n*<sub>bio</sub>, and of C atoms, *n*<sub>C</sub>, that can be acquired by microorganisms in a  
 135 transformation step. An adjusted MTB method is presented below, with description of partial  
 136 growth yield determination.

137 The microbial growth yield is calculated from the anabolic and catabolic yields:

$$\frac{1}{Y} = \frac{1}{Y_{\text{cata}}} + \frac{1}{Y_{\text{ana}}} \quad (1)$$

138 The catabolic yield is determined from the energy of the redox reaction captured by the  
 139 microorganisms:

$$Y_{\text{cata}} = \frac{n_{\text{bio}} \Delta G_r^{m'}}{n \Delta G_{\text{ATP}}^{\text{obs}}} \times Y_{\text{ATP}} \quad (2)$$

140 where *n* is the number of electrons transferred in the redox reaction and *n*<sub>bio</sub> is the number of  
 141 electrons from the redox reaction available to the bacterium for energy generation. Empirically, two



142 electrons are transferred for each C-H bond oxidized;  $n_{\text{bio}}$  thus corresponds to the number of C-H  
 143 bonds present in the substrate minus the number of C-H bonds in the formed metabolite.  $\Delta G_r^{m'}$  is  
 144 the Gibbs free energy of the redox reaction at metabolic conditions (1 mmol L<sup>-1</sup> chemical activity,  
 145 0.1 mol L<sup>-1</sup> ionic strength and pH 7).<sup>45</sup>  $\Delta G_{\text{ATP}}^{\text{obs}}$  is the observed Gibbs energy needed to synthesize  
 146 adenosine triphosphate (ATP, approx. 80 kJ mol<sup>-1</sup>) for typical conditions inside a microbial cell,  
 147 calculated from a  $\Delta G$  value of 31.8 kJ/mol<sup>46</sup> divided by the microbial efficiency of 40%,<sup>47</sup>  $Y_{\text{ATP}}$  is the  
 148 biomass yield on ATP (default 5 g cell dw mol<sup>-1</sup> ATP for non-sugar substrates).<sup>47</sup>

149 The anabolic yield ( $Y_{\text{ana}}^{\text{C}}$ ) is determined from the amount of C in the substrate available for the  
 150 synthesis of new biomass:

$$Y_{\text{ana}}^{\text{C}} = \frac{n_{\text{C}} M_{\text{C}}}{\sigma_{\text{C}}} \quad (3)$$

151  $n_{\text{C}}$  is the moles of C acquired by the microorganisms in the transformation [mol],  $M_{\text{C}}$  is the molar  
 152 mass of C [g mol<sup>-1</sup>], and  $\sigma_{\text{C}}$  is the fraction of C in the dry cell [g C<sub>cell</sub> g<sup>-1</sup> cell dw].

153 Furthermore, the anabolic yield can also be dependent on other limiting substrates such as N  
 154 ( $Y_{\text{ana}}^{\text{N}}$ ):

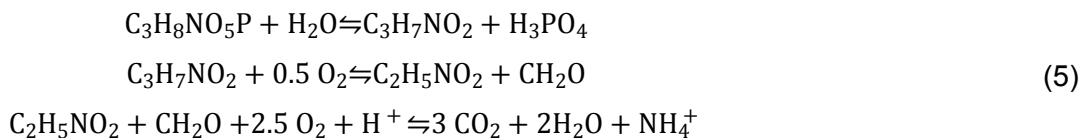
$$Y_{\text{ana}}^{\text{N}} = \frac{n_{\text{N}} M_{\text{N}}}{\sigma_{\text{N}}} \quad (4)$$

155 where the subscript  $N$  refers to N. For a microbial cell stoichiometry of C<sub>5</sub>H<sub>7</sub>O<sub>2</sub>N ( $n_{\text{C,cell}} = 5$  mol C  
 156 per mol cell), 1 mol cell is 113 g (labeled N and C 119 g/mol),  $\sigma_{\text{C}}$  is 0.531 g C<sub>cell</sub> g<sup>-1</sup> cell dw and  $\sigma_{\text{N}}$   
 157 is 0.124 g N<sub>cell</sub> g<sup>-1</sup> cell dw.<sup>48</sup>

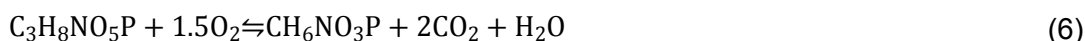
158 **Flux of carbon, nitrogen, energy and electrons.** Glyphosate (C<sub>3</sub>H<sub>8</sub>NO<sub>5</sub>P) is biodegraded via two  
 159 pathways: (i) the sarcosine pathway and (ii) the AMPA pathway.<sup>36-38</sup> All three C atoms and the N  
 160 atom can be incorporated into cellular biomass (Figure S1) or released as fully oxidized C in CO<sub>2</sub>  
 161 and fully reduced N in ammonium (NH<sub>4</sub><sup>+</sup>). The oxidation state of N in glyphosate is -3,  
 162 corresponding to its oxidation state in ammonium and amines. The oxidation state of P in GLP is  
 163 +3 as it is a phosphonate.<sup>49</sup> The average oxidation state of the C atoms in GLP is +2/3. Also, when  
 164 the phosphonate is oxidized to orthophosphate (+5) two electrons are released and the C in  
 165 sarcosine is reduced to an oxidation state of 0. In total, the complete mineralization of glyphosate  
 166 releases 12 electrons (see SI S2 for details).

167 **Sarcosine pathway.** Glyphosate is initially transformed into equimolar amounts of sarcosine  
 168 (C<sub>3</sub>H<sub>7</sub>NO<sub>2</sub>) and orthophosphate through cleavage of the C-P bond by C-P lyase.<sup>36</sup> Sarcosine is  
 169 immediately transformed into equimolar quantities of formaldehyde (CH<sub>2</sub>O) and glycine (C<sub>2</sub>H<sub>5</sub>NO<sub>2</sub>),

170 in which both labels were found.  $^{13}\text{C}$  and  $^{15}\text{N}$  co-labelled glycine is thus evidence for the sarcosine  
 171 pathway.<sup>36</sup> Formaldehyde and glycine are either incorporated into biomass or oxidized to  $\text{CO}_2$ . The  
 172 full mineralization of glyphosate via the sarcosine pathway can be formulated as:



173 **AMPA pathway.** Glyphosate is oxidized to glyoxylate ( $\text{CHOCOO}^-$ ) and AMPA ( $\text{CH}_6\text{NO}_5\text{P}$ ) through  
 174 cleavage of the C-N bond by, e.g., glyphosate oxidoreductase.<sup>36</sup> The C in AMPA has an oxidation  
 175 state of 0 while the C in glyoxylate has an oxidation state of +2. AMPA and glyoxylate can further  
 176 be metabolized to biomass or  $\text{CO}_2$ . According to the results of the glyphosate turnover  
 177 experiment<sup>38</sup>, we assume that AMPA is an accumulating metabolite retaining N and P and only C  
 178 in glyoxylate is mineralized. The reaction describing the degradation via the AMPA pathway takes  
 179 the following form:



180

181 **Partial growth yields, biomass, metabolites and  $\text{CO}_2$  formation.** The MTB approach also  
 182 includes a C mass balance method to calculate the formation of bioNER.<sup>20</sup> A modified method  
 183 capable of considering competing transformation pathways, leading to both  $\text{CO}_2$  and accumulating  
 184 metabolites, is presented below.

185 The moles of C in glyphosate degraded via the AMPA pathway results in the formation of  $Y_{\text{AMPA}}^{\text{C}}$   
 186 moles of biomass C per mol glyphosate C ( $\text{mol C (mol C)}^{-1}$ ),  $n_{\text{ox}}$  moles of  $\text{CO}_2$  per mol glyphosate  
 187 C ( $\text{mol C (mol C)}^{-1}$ ), and  $C_{\text{AMPA}}$  moles of C in AMPA ( $\text{mol C}$ ):

$$C_{\text{GLP}} = \underbrace{Y_{\text{AMPA}}^{\text{C}} \times C_{\text{GLP}}}_{\text{X formed}} + \underbrace{n_{\text{ox}} \times C_{\text{GLP}}}_{\text{CO}_2 \text{ formed}} + \underbrace{C_{\text{AMPA}}}_{\text{AMPA formed}} \quad (7)$$

188 where  $C_{\text{GLP}}$  is moles of C in glyphosate. Normalizing with  $C_{\text{GLP}}$  gives (in units  $\text{mol C (mol C)}^{-1}$ ):

$$1 = Y_{\text{AMPA}}^{\text{C}} + n_{\text{ox}} + \frac{C_{\text{AMPA}}}{C_{\text{GLP}}} = Y_{\text{AMPA}}^{\text{C}} + n_{\text{ox}} + \frac{1}{3} \quad (8)$$

189 Glyphosate degraded via the sarcosine pathway results in the formation of  $Y_{\text{SRC}}^{\text{C}}$  moles of biomass  
 190 C and  $(1 - Y_{\text{SRC}}^{\text{C}})$  moles of  $\text{CO}_2$  and the mass balance is simply:

$$C_{\text{GLP}} = \underbrace{Y_{\text{SRC}}^{\text{C}} \times C_{\text{GLP}}}_{\text{X formed}} + \underbrace{(1 - Y_{\text{SRC}}^{\text{C}}) \times C_{\text{GLP}}}_{\text{CO}_2 \text{ formed}} \quad (9)$$

191 One can calculate  $Y_{\text{AMPA}}^{\text{C}}$  and  $Y_{\text{SRC}}^{\text{C}}$  and the moles of glyphosate degraded via the AMPA pathway  
 192 are measured (equal to the moles of AMPA formed), thus the total amount of biomass and  $\text{CO}_2$   
 193 formed can be found from the sum of biomass and  $\text{CO}_2$  formed via both pathways:

$$\text{Total CO}_2 = \underbrace{n_{\text{ox}} \times C_{\text{GLP}}^{\text{AMPA}}}_{\text{AMPA pathway}} + \underbrace{(1 - Y_{\text{SRC}}^{\text{C}}) \times C_{\text{GLP}}^{\text{SAR}}}_{\text{Sarcosine pathway}} \quad (10a)$$

$$\text{Total biomass} = \underbrace{Y_{\text{AMPA}}^{\text{C}} \times C_{\text{GLP}}^{\text{AMPA}}}_{\text{AMPA pathway}} + \underbrace{Y_{\text{SRC}}^{\text{C}} \times C_{\text{GLP}}^{\text{SAR}}}_{\text{Sarcosine pathway}} \quad (10b)$$

194 where  $C_{\text{GLP}}^{\text{SAR}}$  and  $C_{\text{GLP}}^{\text{AMPA}}$  denote the moles of glyphosate degraded via either pathway. The total  
 195 amount of biomass includes both living and dead biomass, i.e., the bioNER formed.

196 **Model structure.** The test system was described as a multi-compartment model including mass  
 197 transfer between water and sediment. Based on the experimental results, only glyphosate and  
 198 AMPA were explicitly considered in the model, while other intermediates were assumed to be  
 199 readily susceptible to biodegradation. State variables were: mass of glyphosate in supernatant  
 200 water ( $W$ ), pore water ( $D$ ), sediment ( $A$ ), sequestered ( $S$ ); mass of AMPA in supernatant water,  
 201 pore water, sediment; microbial biomass in sediment ( $X$ ); mass of  $\text{CO}_2$ . The  $^{13}\text{C}/^{15}\text{N}$  ratio of the  
 202 NER was  $>3$  (except at the final measurement), indicating that the amount of NER formed from  
 203 AMPA (C/N equal to 1) was negligible and thus assumed to not occur.

204 The experimental system was unstirred, hence exchanges between compartments were controlled  
 205 by diffusive transport.<sup>3</sup> Exchange between the supernatant water and the sediment pore water  
 206 were described as diffusion through an unstirred boundary layer and to a sediment depth of 1 mm,  
 207 based on the calculated depth of diffusion within 80 days<sup>50</sup> (see also SI S4) and penetration depth  
 208 of  $\text{O}_2$ .<sup>7</sup> Biodegradation was assumed to occur only for glyphosate dissolved in the sediment pore  
 209 water ( $D$ ), as negligible formation of AMPA and  $\text{CO}_2$  was observed in experiments containing only  
 210 the creek water used in the experiment.<sup>38</sup> Exchange processes were described with well-  
 211 established first-order kinetics,<sup>11,20</sup> hence, only the equations related to the biodegradation of  
 212 glyphosate, microbial growth and formation of bioNER are presented in detail. Calculations were  
 213 made in the unit  $\mu\text{mol}$  compound. All the model equations can be found in the SI S4, and all input  
 214 data are listed in Table S5. A schematic overview of the model compartments is shown in Figure  
 215 S2b. Seven model parameters together with the associated model uncertainty were estimated  
 216 using the Bayesian optimization method DiffeRential Evolution Adaptive Metropolis algorithm  
 217 (DREAM).<sup>51</sup> Details can be found in the SI S5.

218 **Biodegradation of glyphosate.** The experimental data show that glyphosate was a source of both  
 219 N and C as  $^{13}\text{C}$  and  $^{15}\text{N}$  were incorporated into amino acids of proteins, and thus also into microbial  
 220 biomass. The N/P ratio in microbial biomass is 13:1 on a molar basis,<sup>52</sup> while in glyphosate it is 1:1.

221 We can therefore safely assume that N is limiting anabolism before P, unless there are external N  
 222 sources available.. The ratio of C/N in microbial biomass is 5:1, while it is 3:1 in glyphosate. Thus,  
 223 once N and P supply is secured by degradation of glyphosate via the sarcosine pathway, only C is  
 224 limiting microbial anabolism, also because a large fraction of C must be oxidized to CO<sub>2</sub> for the  
 225 energy gain (catabolism). Degradation via the AMPA pathway does not provide N nor P for the  
 226 degrader but it provides glyoxylate, an excellent C and energy source. Therefore, the observed  
 227 shift in pathways, as indicated by the accumulation of AMPA, must be modulated by changes of  
 228 the substrate needs. Filling the pools of N or P in the degrading microorganisms combined with  
 229 energy limitations may signal the metabolic shift. In order to reflect the experimental results of the  
 230 degradation through the AMPA pathway was thus modeled as a being dually limited, i.e. the  
 231 respective transformation rate is dependent upon the N from the sarcosine pathway incorporated  
 232 into the biomass and down-regulated as long as N is limiting. The metabolic fluxes for glyphosate  
 233 degradation through the sarcosine and AMPA pathway are described using *Michaelis-Menten*  
 234 kinetics:

$$\frac{dn_{M, SRC}}{dt} = v_{max, SRC} \frac{a_D}{a_D + K_{S, SRC}} X \quad (11)$$

235

$$\frac{dn_{M, AMPA}}{dt} = v_{max, AMPA} \frac{a_D}{a_D + K_{S, AMPA}} \frac{a_D^N}{a_D^N + K_S^N} X \quad (12)$$

236 where  $n_M$  [μmol] is the metabolized amount of glyphosate,  $X$  is the amount of degrader microbes  
 237 [μmol bacteria],  $v_{max}$  [μmol (μmol bacteria d)<sup>-1</sup>] is the maximum transformation rate and  $K_S$  [μmol  
 238 L<sup>-1</sup>] is the half-saturation constant for glyphosate through the sarcosine and AMPA pathway  
 239 (subscript SRC and AMPA, respectively), and the N released from the sarcosine pathway  
 240 (superscript N),  $a_D$  is the chemical activity of glyphosate or AMPA (equivalent to the freely  
 241 dissolved concentration, μmol L<sup>-1</sup>) in sediment pore water (index D). The chemical activity of  
 242 dissolved inorganic N  $a_D^N$  is calculated from the NH<sub>4</sub><sup>+</sup> released during mineralization of glyphosate  
 243 through the sarcosine pathway resulting in potential turnover inhibition.

244 **Biomass formation.** Microbial growth was described by *Monod* kinetics including a term for  
 245 microbial decay (similar to previous studies<sup>11,53,54</sup>):

$$\frac{dX}{dt} = Y_{SRC} \times \frac{dn_{M, SRC}}{dt} + Y_{AMPA} \times \frac{dn_{M, AMPA}}{dt} - b \times X \quad (13)$$

246 where the first two terms consider microbial growth and the last term considers microbial decay.  
 247  $Y_{SRC}$  and  $Y_{AMPA}$  [μmol bacteria (μmol substrate)<sup>-1</sup>] are microbial growth yields of the sarcosine and

248 AMPA pathways, respectively,  $dn_{M,SRC}/dt$  and  $dn_{M,AMPA}/dt$  are the metabolic fluxes, and  $b$  [ $d^{-1}$ ] is a  
249 first-order rate constant of microbial decay.

250 Microbial necromass,  $X_{necro}$  [ $\mu\text{mol}$  bacteria], is formed by the decay of living biomass  $X$  and is  
251 subject to slow mineralization with rate constant  $k_m$  [ $d^{-1}$ ], here set to  $0.001 d^{-1}$  comparable to that of  
252 soil organic matter:<sup>11</sup>

$$\frac{dX_{necro}}{dt} = b \times X - k_m \times X_{necro} \quad (14)$$

253 Living bacterial mass and necromass both contribute to the formation bioNER:

$$\frac{dbioNER}{dt} = \frac{dX}{dt} + \frac{dX_{necro}}{dt} \quad (15)$$

254 Microbial growth has been monitored by stable isotope incorporation into amino acids/proteins of  
255 living biomass.<sup>16,17,19,38,55,56</sup> To calculate the total label incorporation into other biomolecules than  
256 amino acids, a factor of 2 has usually been applied to calculate the biomass and bioNER resp.,  
257 from measured amino acids ( $\sim 50\%$  of a dry cell is proteins<sup>57</sup>).<sup>9</sup>

258 **Carbon dioxide.**  $\text{CO}_2$  was assumed to originate from the mineralization of glyphosate via both  
259 pathways and from microbial necromass:

$$\frac{dn_{CO_2}}{dt} = (1 - Y_{SRC}^C) \frac{dn_{M,SRC}}{dt} n_{C,SRC} + (1 - Y_{AMPA}^C) \frac{dn_{M,AMPA}}{dt} n_{C,AMPA} + k_m X_{necro} n_{C,cell} \quad (16)$$

260 These calculations refer to a C basis:  $n_{CO_2}$  [ $\mu\text{mol}$ ] is the amount of formed  $\text{CO}_2$ . Three moles C are  
261 metabolized via the sarcosine pathway (with  $n_{C,SRC}$  is 3 mol C per mol glyphosate) and only two  
262 moles C via the AMPA pathway (with  $n_{C,AMPA}$  is 2 mol C per mol glyphosate), since AMPA  
263 accumulates.  $Y_{SRC}^C$  and  $Y_{AMPA}^C$  are microbial growth yields (moles of C in bacteria per moles of C  
264 in substrate, or  $\text{g C g}^{-1} \text{C}$ ).<sup>20</sup>

265

## 266 3 Results

267 **Microbial growth yield estimates of glyphosate degradation.** Table 1 shows the calculated  
268 microbial growth yields and thermodynamic analysis of the different pathways. Negative  $\Delta G_r^{m'}$   
269 values indicate exothermic, energetically favorable, reactions. The first step of the sarcosine  
270 pathway (glyphosate  $\rightarrow$  sarcosine) is favorable, while the first step of the AMPA pathway  
271 (glyphosate  $\rightarrow$  AMPA + glyoxylate) is not. If glyoxylate mineralization is included, the reaction is  
272 thermodynamically favorable.  $\Delta G_r^{m'}$  of the mineralization via the sarcosine pathway is more than  
273 six-fold that of the incomplete AMPA pathway, which is also reflected in the estimated growth  
274 yields. The difference between  $Y_{ana}^C$  and  $Y_{ana}^N$  shows that glyphosate is a better source of N than

275 of C for microbial growth, indicating that C is the limiting substrate. For the sarcosine pathway, the  
276 majority of the microbial yield is associated to metabolism of glycine and formaldehyde. The  
277 anabolic contribution is higher than the catabolic contribution ( $Y_{ana}^C > Y_{cata}$ ). In the AMPA pathway,  
278 most of the potential energy and the N mass are retained in AMPA. If AMPA is an accumulating  
279 metabolite (as seen in this study), then only glyoxylate metabolism provides C and energy.  
280 However, the question remains open why AMPA is not degraded under the test conditions,  
281 although its mineralization seems very energetically favorable, see discussion.

282 **Table 1.** Estimated microbial growth yields of the different degradation steps in the sarcosine and AMPA pathways.

	$\Delta G_r^{m'}$	$n_{bio}/n$	C-H bonds cleaved	$Y_{ana}^N$	$Y_{ana}^C$	$Y_{cata}$	$Y^C$	$Y^C$
	$\text{kJ mol}^{-1}$			$\text{g bac mol}^{-1}$	$\text{g bac mol}^{-1}$	$\text{g bac mol}^{-1}$	$\text{g bac mol}^{-1}$	$\text{g C g}^{-1} \text{C}$
<b>Sarcosine pathway</b>								
Glyphosate -> sarcosine + P <sub>i</sub>	-90	0/0	0	0	0	0	0	0
Sarcosine -> glycine + formaldehyde	-182	2/2	1	0	0	11.4	0	0
Glycine -> 2 CO <sub>2</sub>	-708	4/6	2	119	47.6	29.5	18.2	0.38
Formaldehyde -> CO <sub>2</sub>	-500	4/4	2	0	23.8	31.2	13.5	0.57
<b>AMPA pathway</b>								
Glyphosate -> AMPA + glyoxylate	247	2/2	1	0	0	<0	0	0
AMPA -> CO <sub>2</sub>	-1211	4/6	2	119	23.8	50.5	16.2	0.68
Glyoxylate -> 2 CO <sub>2</sub>	-515	2/4	1	0	47.6	16.1	12.0	0.25
<b>Used for calculation</b>								
Glyphosate -> 3 CO <sub>2</sub>	-1480	8/12	4	119	71.4	61.7	33.1	0.46
Glyphosate -> AMPA + 2 CO <sub>2</sub>	-268	4/6	2	0	47.6	11.2	9.1	0.19

283 The calculations were done for metabolic conditions (superscript m: for chemical activities of 0.1 mmol L<sup>-1</sup> and ionic strength of 0.1 mol L<sup>-1</sup>) and pH is 7  
284 (superscript ').  $\Delta G_r^{m'}$  is the Gibbs energy of the redox reaction (kJ mol<sup>-1</sup>),  $Y_{ana}^C$  is the anabolic yield on C in the substrate,  $Y_{ana}^N$  is the anabolic yield on N  
285 in the substrate,  $Y_{cata}$  is the catabolic yield gained from the redox reaction,  $Y^C$  is the microbial growth yield if C is the limiting substrate and is calculated  
286 from  $Y_{cata}$  and  $Y_{ana}^C$ . Unit is g bacteria dry weight per mol substrate, except the last column in mol C in bacteria per mol C substrate (g C g<sup>-1</sup> C). 1 mol  
287 bacteria is 119 g (<sup>13</sup>C and <sup>15</sup>N labeled).

288

289 **Model results, uncertainty and parameter identifiability.** The seven calibrated input parameters  
 290 and their quality criteria (credibility interval, coefficient of variation  $\sigma/\mu$ , maximum absolute  
 291 correlation coefficient  $r$ ) are shown in Table 2. Only  $X(0)$  and  $K_{OC,GLP}$  can be considered identifiable  
 292 based on the criteria by Frutiger et al.<sup>58</sup> ( $r < 0.7$ ,  $CV = \sigma/\mu < 0.5$ ), due to the high positive  
 293 correlation between the  $v_{max}$ -values and their accompanying  $K_S$ -values.

294 **Table 2:** Result of the DREAM parameter optimization. The set of parameters resulting in the maximum a-  
 295 posterior probability are listed together with their 95% credibility interval (CI), the coefficient of variation CV  
 296 ( $\sigma/\mu$ ) and the maximum absolute correlation coefficient (abs  $r$  (max)).

Parameter	Unit	Optimum (95% CI)	CV	abs $r$ (max)
$v_{max, SRC}$	$\mu\text{mol glyphosate } (\mu\text{mol bacteria d})^{-1}$	2.56 (0.47; 3.45)	0.39	0.87
$K_{S, SRC}$	$\mu\text{mol glyphosate L}^{-1}$	391 (52.0; 395)	0.35	0.87
$K_{OC, GLP}$	$\text{L kg}_{OC}^{-1}$	882 (769; 1093)	0.09	0.28
$v_{max, AMPA}$	$\mu\text{mol glyphosate } (\mu\text{mol bacteria d})^{-1}$	26.9 (8.71; 29.6)	0.30	0.89
$K_{S, AMPA}$	$\mu\text{mol glyphosate L}^{-1}$	1327 (431; 1484)	0.29	0.89
$K_{S, N}$	$\mu\text{mol glyphosate L}^{-1}$	47.0 (3.34; 76.9)	0.56	0.50
$X(0)$	$\mu\text{mol bacteria L}^{-1}$	0.050 (0.021; 0.13)	0.45	0.55

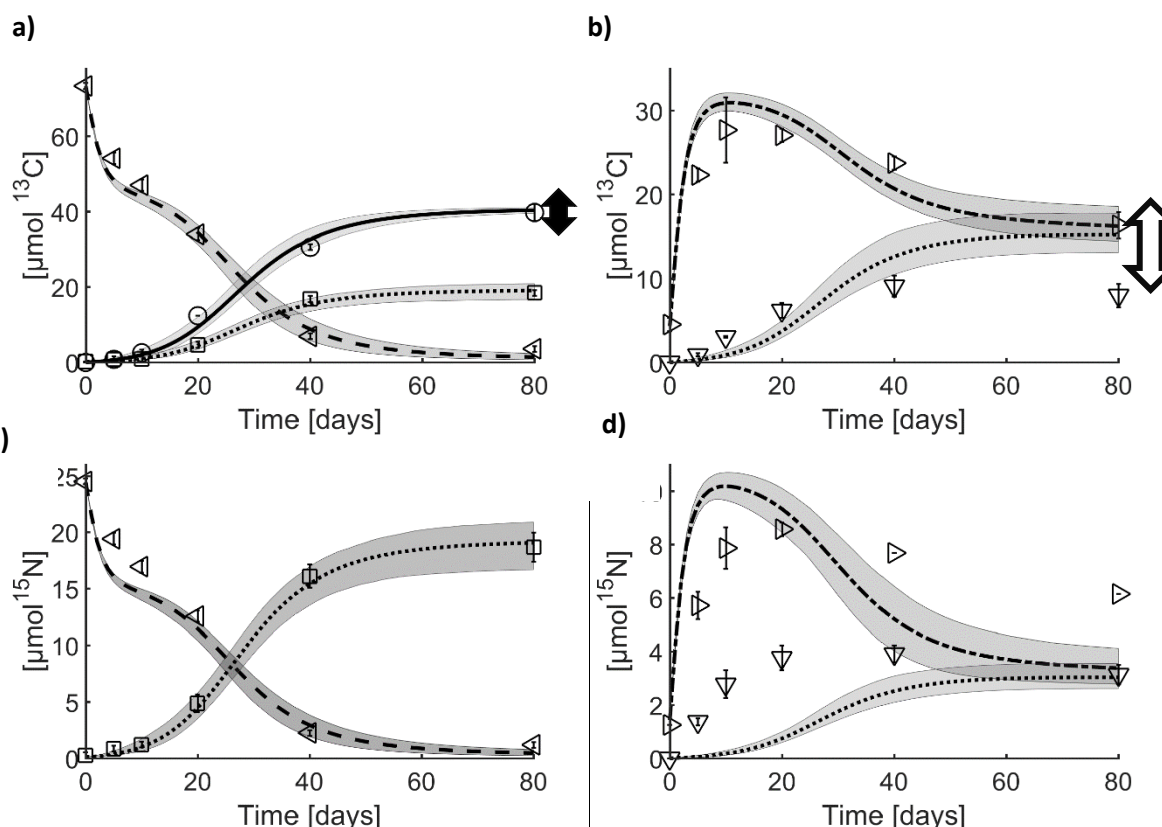
297

298 Simulation results for both  $^{13}\text{C}$  and  $^{15}\text{N}$  are shown and compared to experimental data in Figure 1.  
 299 The degradation of glyphosate, formation of AMPA, formation of NER, and formation of  $\text{CO}_2$  are  
 300 captured very well (RMSE 2.2). Simulated  $^{13}\text{C}$  in bioNER was lower than the  $^{13}\text{C}$ -total amino acids  
 301 until day 40, while simulated  $^{15}\text{N}$  in bioNER was strikingly lower than the  $^{15}\text{N}$ -total amino acids  
 302 measured at all times. Obviously,  $^{13}\text{C}$  and  $^{15}\text{N}$  were not incorporated into biomass in the expected  
 303 C/N ratio of 5:1. The initial difference between bioNER and total NER is three times higher on a  $^{13}\text{C}$   
 304 basis than on a  $^{15}\text{N}$  basis (Figure 1b,d), and it is likely that it is sequestered glyphosate. In addition,  
 305 measured  $^{15}\text{N}$  in total amino acids is much higher than the simulated bioNER, indicating that N is  
 306 intermediately enriched in the biomass and not released as  $\text{NH}_4^+$ , thus N is presumably the control  
 307 factor. Remarkably, the use of the simple modified carbon mass balance gives in general similar  
 308 final values for bioNER (total biomass) and  $\text{CO}_2$  (shown as arrows in Figure 1a,b).

309



310



311

312

313

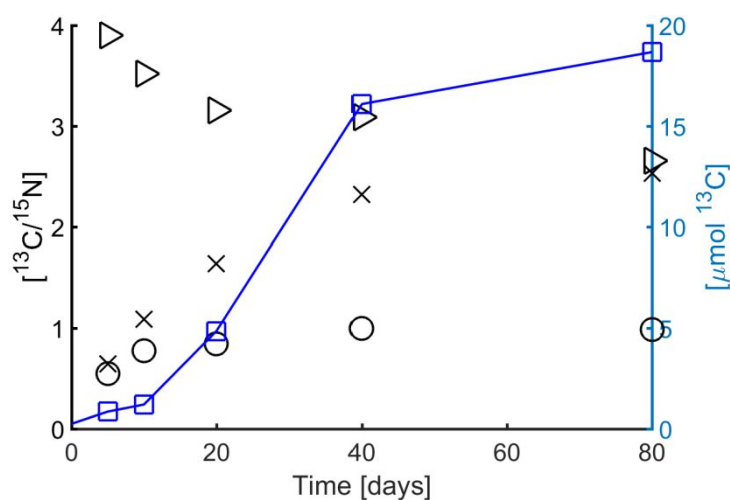
314 **Figure 1.** Model simulations using the optimized parameter set determined using DREAM. Results shown in  
 315  $\mu\text{mol } ^{13}\text{C}$  (a,b) and  $\mu\text{mol } ^{15}\text{N}$  (c,d). Lines are model simulations and symbols are measurements. Vertical  
 316 bars indicate the standard deviation of the measurements. **(a,c)** Extractable fractions of glyphosate (---;  $\triangleleft$ ),  
 317 AMPA (---;  $\square$ ) and  $\text{CO}_2$  (—;  $\circ$ ); **(b,d)** Formation of simulated and measured total NER (---;  $\triangleright$ ), measured  
 318 total amino acids ( $\nabla$ ) and simulated bioNER (...). The grey bands delineate the 95% credibility interval of  
 319 the model simulations. The vertical arrows in panels (a) and (b) show the upper and lower bounds of the  
 320 formed amounts of  $\text{CO}_2$  (black) and bioNER (white) calculated using the modified MTB carbon balance  
 321 method (see SI S8 for details).

322

323  **$^{13}\text{C}/^{15}\text{N}$ -ratio.** Co-labeling with  $^{13}\text{C}$  and  $^{15}\text{N}$  allowed calculating observed  $^{13}\text{C}/^{15}\text{N}$  ratios in amino  
 324 acids and NER over the duration of the experiment. The measured  $^{13}\text{C}/^{15}\text{N}$  ratios in total amino  
 325 acids, NER, and amino acids in living cells are shown in Figure 2 together with the formation of  
 326 AMPA. The  $^{13}\text{C}/^{15}\text{N}$  ratios in amino acids in living cells and total amino acids were initially  $<1$ , with  
 327 the ratio in amino acids in living cells converging to approximately 1 at the end of the experiment.  
 328 The  $^{13}\text{C}/^{15}\text{N}$ -ratio in total amino acids increased concomitantly with the formation of AMPA to a  
 329 maximum of 2.6, while the average C/N ratio of amino acids in living cells is 3.7:1 (Table S2). This

330 shows that  $^{15}\text{N}$  was initially incorporated into amino acids to a larger extent than  $^{13}\text{C}$ . As glyphosate  
331 is an aminophosphonic acid analog of glycine, it is not surprising that  $^{13}\text{C}$  and  $^{15}\text{N}$  were  
332 predominately found in glycine (60% of the  $^{13}\text{C}$  and 34% of the  $^{15}\text{N}$  measured in total amino acids  
333 on day 5).<sup>38</sup> The  $Y^{\text{C}}$  for the sarcosine pathway (Table 1) is 0.46, i.e. 54% of C forms  $\text{CO}_2$  if  
334 glyphosate is the sole C source. However, the measured  $^{13}\text{CO}_2/^{13}\text{C}$ -total amino acids ratio was  $<1$   
335 until day 20 (Fig. 2). After day 20, when the AMPA pathway dominates, only  $^{13}\text{C}$  was incorporated  
336 in amino acids, and the  $^{13}\text{C}/^{15}\text{N}$ -ratio in total amino acids rose above 1. In the NER, the  $^{13}\text{C}/^{15}\text{N}$ -  
337 ratio was  $>3$  in all measurements except the last (80 days). At the end of the experiment, the  
338  $^{13}\text{C}/^{15}\text{N}$  ratios in NER and in total amino acids were similar, suggesting that the NER are  
339 predominately biogenic, which is supported by the model simulations. Therefore, the modeling  
340 approach reflecting the experimental data conclusively shows that C is limiting or the excess of N  
341 is triggering the shift from sarcosine pathway towards AMPA formation.

342



343

344 **Figure 2.**  $^{13}\text{C}/^{15}\text{N}$  ratio measured in the experiment. Left axis:  $^{13}\text{C}/^{15}\text{N}$  ratio in the measured total amino acids  
345 ( $\times$ ), living amino acids ( $\circ$ ), and non-extractable residues (NER) ( $\triangleright$ ) over time. Right axis (blue): Measured  
346 AMPA in  $\mu\text{mol}$  ( $\square$ ).

347

348

#### 349 4 Discussion

350

351 The primary goal of the present study was to extend and validate the microbial growth yield  
352 estimation (MTB) method combined with the ‘unified model for biodegradation and sorption’ in  
353 order to capture the phenomena of various transformation pathways with metabolite formation and  
354 multi-substrate use for optimized interpretation of OECD 308 (and also 307) test systems. This was  
355 performed for a  $^{13}\text{C}$  and  $^{15}\text{N}$  co-labeled glyphosate degradation experiment<sup>38</sup>. Glyphosate  
356 consumption, formation of metabolites (AMPA) and biomolecules, as well as energy gain and  
357 distribution of  $^{13}\text{C}$  and  $^{15}\text{N}$  were successfully modeled and the metabolic fluxes and element  
358 availability were assessed. Anabolic yield calculations conditioned on the microbial C and N  
359 demands gave insights into nutrient limitations and were confirmed by the measured  $^{13}\text{C}/^{15}\text{N}$  ratios.  
360 The results showed that glyphosate mineralization via the sarcosine pathway gave a higher growth  
361 yield than via the (incomplete) AMPA pathway. However, in a later stage of degradation the  
362 release of AMPA may protect the cells from N overflow which may cause the accumulation of this  
363 transformation product. The extended modeling methods allow improved interpretations and  
364 hypothesis derivation for transformation pathways in environmental fate test systems by  
365 considering the bioenergetic feasibility and influential factors, such as nutrient limitation and  
366 element distribution.

367 **Model performance.** The model simulations were able to fully capture the experimental  
368 elimination of glyphosate and the concurrent formation of total NER, AMPA and  $\text{CO}_2$  observed in  
369 the OECD 308 setup. However, the formation of biomass as observed by amino acid analysis was  
370 only partly reflected. This is caused by the analytical bias introduced when biomass formation is  
371 calculated from amino acid analysis of hydrolyzed microbial proteins (SI S3). While other model  
372 structures<sup>3,6,8</sup> have been used to capture the dynamics of the OECD 308 test system and formation  
373 of NER they do not provide any information regarding the biomass formation, NER composition,  
374 and macro-element distribution. The prediction of the NER composition, in particular the bioNER  
375 contribution, requires the mechanistic description of microbial growth and decay in the model.

376 The calibration procedure resulted in acceptable uncertainty ranges of the estimated parameters  
377 and model output (Table 2 and Figure 1). The maximum specific growth rate found for the AMPA  
378 pathway ( $\mu_{\text{max, AMPA}}$  2.04  $\text{d}^{-1}$ ) is comparable to previously reported findings, while, the one  
379 determined for the sarcosine pathway ( $\mu_{\text{max, SRC}}$  0.71  $\text{d}^{-1}$ ) is lower.<sup>36</sup> However, direct comparison is  
380 difficult due to the difference in the measurement units reported. The determined affinity constant  
381  $K_{\text{S, SRC}}$  (391  $\mu\text{mol L}^{-1}$ ) is higher than the ranges reported for *Pseudomonas* sp. strain PG2982 (23  
382  $\mu\text{mol L}^{-1}$ ) and *Arthrobacter* spp. (105–125  $\mu\text{mol L}^{-1}$ ).<sup>32,59</sup> For soil microcosms the value was  
383 estimated to be 412–4050  $\mu\text{mol L}^{-1}$ .<sup>60</sup> The value obtained for  $K_{\text{S, N}}$  is within the affinity data  
384 compiled for ammonia elsewhere.<sup>61</sup>

385 **Shift of transformation pathways.** From a thermodynamic perspective, the sarcosine pathway is  
386 preferable to the AMPA pathway (Table 1) and gives access to the nutrients N and P, although in  
387 an over-stoichiometric relation in comparison to microbial biomass. However, the experimental  
388 data show that microorganisms favored the AMPA pathway after day 10. Based on the macro-  
389 element availability in glyphosate, we hypothesized that P is in surplus in this molecule and that N  
390 saturation and C deficit modulated the switch of pathways leading to the formation of AMPA. The  
391 calculated  $Y_{ana}^N$  is 1.7 times higher than  $Y_{ana}^C$ , further indicating that C is limiting the anabolism.  
392 Microorganisms thus need to support their growth by using other C sources than glyphosate, since  
393 the glyphosate degradation via the sarcosine pathway forms  $CO_2$  resulting in  $NH_4^+$  release and  
394 overflow in the living cells. Once sufficient N is available from the sarcosine pathway due to C  
395 mineralisation, the faster formation of AMPA dominates and prevents the cells from internal  
396 ammonia-N overflow. This may be an explanation for the AMPA accumulation under the batch  
397 conditions of the OECD test 308 and other batch test systems and also explain AMPA occurrence  
398 in the environment due to slower AMPA turnover.<sup>62</sup> Similar results were found for glyphosate in  
399 OECD 307 fate studies in soil but with lower amounts of microbial biomass.<sup>63</sup> Also, the sarcosine  
400 pathway is more costly in terms of enzyme synthesis (C-P lyase), which may cause slower  
401 substrate turnover and growth of microorganisms than the AMPA pathway (see  $v_{max}$  and  $\mu_{max}$   
402 values, Table 2 and Table S5).

403 The  $^{13}C/^{15}N$  ratio measured in amino acids is much lower than 3:1 (in glyphosate) until day 40,  
404 which indicates the use of non-glyphosate C sources for anabolism and challenges the assumption  
405 of single substrate use and stable isotope probing approaches in general.<sup>64</sup> Under the batch  
406 conditions of OECD 308 test, but presumably also in soils (OECD 307), the initial mixing and  
407 rewetting of the sediment can make organic matter available as substrate and lead to an initial  
408 burst of (non-labeled)  $CO_2$  (Birch effect).<sup>65</sup> When this initial effect is gone, starvation will prevail and  
409 may also trigger a shift in the glyphosate degradation pathways, particularly under C limitations.  
410 The use of other C sources without a considerable impact on catabolism or anabolism may be  
411 explained by the mining of microbial building blocks by the degrader microorganisms with minimal  
412 energetic impact on the anabolism. These building blocks can be derived from microbial  
413 necromass always present in sediments and soils. Additional C sources have consequences for  
414 the amount of living biomass when calibrated to measured amino acids, and for the fitted maximum  
415 rate ( $v_{max} \cdot X$ ). We therefore excluded the measurements of amino acids hydrolyzed from proteins  
416 in the model calibration. However, these were used to assess biomass and bioNER formation. In  
417 SI S3, theoretically sound conversion factors are derived to convert measurements of  $^{13}C$ - or  $^{15}N$ -  
418 amino acids into total biomass. “Apparent” conversion factors can be calculated by dividing the  
419 simulated  $^{13}C$ - or  $^{15}N$ -bacterial biomass with the measured  $^{13}C$ - or  $^{15}N$ -total amino acids (Figure 1).

420 The "apparent" conversion factors not only varied in time, they were also much lower than the  
421 theoretical factors for glyphosate as sole substrate derived in SI S3 and the commonly applied  
422 factor of 2.<sup>12</sup> For N, the apparent factor was as low as 0.16 and increased to 0.97 by the end of the  
423 experiment. For C it increased from 0.33 to 1.9. This further indicates that N is predominately used  
424 in amino acid synthesis and is stored within the cells whereas C is not. Consequently, the  
425 theoretical conversion factors and the commonly applied factor of 2 are not valid under the  
426 observed conditions. Consequently, the use of these leads to the overestimation of bioNER early in  
427 the simulation test.

428 Hypothetically, the shift in transformation pathways could be caused by both N and P releases.  
429 Low intracellular orthophosphate ( $P_i$ ) concentrations have been shown to enhance the activity of  
430 the enzymatic complex (C-P lyase) of the sarcosine pathway while high concentrations are  
431 inhibitory.<sup>35,37</sup> The maximum concentration of  $P_i$  in the top 1 mm pore water (= boundary layer,  
432 assuming that 90% of all glyphosate- $P_i$  is released)<sup>59</sup> and overlying water is  $78 \mu\text{mol L}^{-1}$ , which is  
433 similar to the inhibition coefficients ( $K_i$ ) reported ( $24\text{--}253 \mu\text{mol L}^{-1}$ ) and may explain the inhibition  
434 of the sarcosine pathway.<sup>31,60</sup> The concentration is however much lower than the inhibition  
435 coefficient reported for the mutant strain GLP-1/Nit-1 ( $2,300 \mu\text{mol L}^{-1}$ ).<sup>31</sup> In addition,  $P_i$  competes  
436 with glyphosate for sorption sites, indicating that it does not remain in solution<sup>66</sup> and thus the P  
437 inhibition hypothesis in the present experiments appears unlikely. This hypothesis together with the  
438 hypothesis that AMPA is degraded has been tested using the model and further information can be  
439 found in SI S6. In Lake Greifensee in Switzerland, the concentration of both glyphosate and AMPA  
440 was observed to decline concomitantly with the depletion of  $P_i$  and a bloom of cyanobacteria.<sup>42</sup>  
441 Cyanobacteria are photoautotrophs, hence, unaffected by the lack of an organic C source. As  
442 some species are also capable of fixing atmospheric N, it is likely that the disappearance of AMPA  
443 and glyphosate in such lakes is driven by a need for P.

444 Considering the C limitation and the less likely impact of P inhibition, N can be identified as the  
445 trigger factor of the shift of degradation pathways to AMPA accumulation. Via the sarcosine  
446 pathway, C is mineralized and eliminated whereas N is not. As shown by the experimental data,  
447  $\text{NH}_4^+$  obviously remains in the degrader cells thus leading to an N overflow within the cells. Thus, it  
448 is justified to hypothesize that the accumulation of AMPA provides a solution to discard excess N  
449 and P and at the same time provide glyoxylate as a C and energy source.

450 **Relevance and research needs.** The 'unified model for biodegradation and sorption' combined  
451 with the extended MTB approach provides a powerful tool for the simulation of biodegradation and  
452 bioNER formation, even in complex experimental settings and with multiple pathways and macro-  
453 element availability. We could show that the developed modeling approach was able to capture

454 water-sediment mass transfer as well as turnover of real experimental data based on yield  
455 estimates for incomplete metabolism. When combined with experiments with multiple isotope  
456 labels in a single substrate,<sup>38</sup> the anabolic yield calculations gave valuable additional insights, in  
457 particular when compared to measured <sup>15</sup>N and <sup>13</sup>C labels, and provided the unique opportunity to  
458 derive hypotheses to explain the shift of microbial degradation and metabolite formation pathways.  
459 The results show that glyphosate degradation is C limited and increasing internal overflow of  
460 ammonia in degrader cells, presumably combined with starvation of the C turnover under the test  
461 conditions, may cause the accumulation of AMPA. One may speculate that in order to avoid AMPA  
462 accumulation when using glyphosate, application of fertilizer and N-rich manure should be applied  
463 only when easily assimilable C sources are available or should be supplied much later than  
464 glyphosate application. Future studies should therefore investigate factors determining the  
465 accumulation of AMPA (being a potential nutritious substrate) for mitigating its occurrence as a  
466 widely observed accumulating metabolite of a generally biodegradable herbicide.

467

468

### 469 **Supporting Information**

470 Data for the calculation of the microbial growth yields; half-reactions describing the transformation  
471 pathways; equations and tables showing how the factors for converting C and N amounts in amino  
472 acids to C and N amounts in bacterial cells were derived; equations for the model implementation;  
473 detailed results of the DREAM parameter inference method; C and N balances.

474

### 475 **Acknowledgements**

476 This collaborative research was financed by general institutional research funds of DTU, UFZ and  
477 TUM. We thank the unknown reviewers for their comments and the resulting improvement of the  
478 manuscript.

479

480

481 **References**

- 482 (1) European Commission. *Regulation (EC) No 1907/2006 - Registration, Evaluation,*  
483 *Authorisation and Restriction of Chemicals (REACH)*; 2006.
- 484 (2) OECD. *Test No. 307: Aerobic and Anaerobic Transformation in Soil*; Paris, 2002.
- 485 (3) Honti, M.; Fenner, K. Deriving Persistence Indicators from Regulatory Water-Sediment  
486 Studies - Opportunities and Limitations in OECD 308 Data. *Environ. Sci. Technol.* **2015**, *49*  
487 (10), 5879–5886.
- 488 (4) European Commission. *Regulation (EC) No 1107/2009 of the European Parliament and of*  
489 *the Council of 21 October 2009 Concerning the Placing of Plant Protection Products on the*  
490 *Market*; 2009.
- 491 (5) ECHA. *Guidance on Information Requirements and Chemical Safety Assessment. Chapter*  
492 *R.11: PBT/VPvB Assessment (Version 3.0)*; Helsinki, Finland, 2017.
- 493 (6) Honti, M.; Hahn, S.; Hennecke, D.; Junker, T.; Shrestha, P.; Fenner, K. Bridging across  
494 OECD 308 and 309 Data in Search of a Robust Biotransformation Indicator. *Environ. Sci.*  
495 *Technol.* **2016**, acs.est.6b01097.
- 496 (7) Shrestha, P.; Junker, T.; Fenner, K.; Hahn, S.; Honti, M.; Bakkour, R.; Diaz, C.; Hennecke,  
497 D. Simulation Studies to Explore Biodegradation in Water–Sediment Systems: From OECD  
498 308 to OECD 309. *Environ. Sci. Technol.* **2016**, *50* (13), 6856–6864.
- 499 (8) Ter Horst, M. M. S.; Koelmans, A. A. Analyzing the Limitations and the Applicability Domain  
500 of Water-Sediment Transformation Tests like OECD 308. *Environ. Sci. Technol.* **2016**, *50*  
501 (19), 10335–10342.
- 502 (9) Kästner, M.; Trapp, S.; Schäffer, A. Consultancy Services to Support ECHA in Improving the  
503 Interpretation of Non-Extractable Residues (NER) in Degradation Assessment. Discussion  
504 Paper - Final Report. Edited by the European Chemical Agency ECHA (June 2018),  
505 available at [www.echa.europa.eu/publications/technical-scientific-reports](http://www.echa.europa.eu/publications/technical-scientific-reports).
- 506 (10) Barriuso, E.; Benoit, P.; Dubus, I. G. Formation of Pesticide Nonextractable (Bound)  
507 Residues in Soil: Magnitude, Controlling Factors and Reversibility. *Environ. Sci. Technol.*  
508 **2008**, *42* (6), 1845–1854.
- 509 (11) Kästner, M.; Nowak, K. M.; Miltner, A.; Trapp, S.; Schäffer, A. Classification and Modelling  
510 of Nonextractable Residue (NER) Formation of Xenobiotics in Soil – A Synthesis. *Crit. Rev.*  
511 *Environ. Sci. Technol.* **2014**, *44* (19), 2107–2171.
- 512 (12) Schäffer, A.; Kästner, M.; Trapp, S. A Unified Approach for Including Non-Extractable  
513 Residues (NER) of Chemicals and Pesticides in the Assessment of Persistence. *Environ.*  
514 *Sci. Eur.* **2018**, *30*, 1–14.
- 515 (13) Barraclough, D.; Kearney, T.; Croxford, A. Bound Residues: Environmental Solution or  
516 Future Problem? *Environ. Pollut.* **2005**, *133* (1), 85–90.
- 517 (14) ECETOC. *Technical Report No. 118 - Development of Interim Guidance for the Inclusion of*  
518 *Non-Extractable Residues (NER) in the Risk Assessment of Chemicals*; Brussels, Belgium,  
519 2013.
- 520 (15) Roberts, T.; Klein, W.; Stillm, G.; Kearney, P.; Drescher, N.; Desmoras, J.; Esser, H.;  
521 Aharonson, N.; Vonk, J. Non-Extractable Pesticide Residues in Soils and Plants. *Pure Appl.*  
522 *Chem.* **1984**, *56* (7), 945–956.
- 523 (16) Nowak, K. M.; Miltner, A.; Gehre, M.; Schäffer, A.; Kastner, M. Formation and Fate of Bound  
524 Residues from Microbial Biomass during 2, 4-D Degradation in Soil. *Environ. Sci. Technol.*  
525 **2011**, *45* (3), 999–1006.
- 526 (17) Nowak, K. M.; Girardi, C.; Miltner, A.; Gehre, M.; Schäffer, A.; Kästner, M. Contribution of  
527 Microorganisms to Non-Extractable Residue Formation during Biodegradation of Ibuprofen  
528 in Soil. *Sci. Total Environ.* **2013**, *445–446*, 377–384.
- 529 (18) Kästner, M.; Nowak, K. M.; Miltner, A.; Schäffer, A. (Multiple) Isotope Probing Approaches to  
530 Trace the Fate of Environmental Chemicals and the Formation of Non-Extractable “bound”  
531 Residues. *Curr. Opin. Biotechnol.* **2016**, *41*, 73–82.
- 532 (19) Poßberg, C.; Schmidt, B.; Nowak, K.; Telscher, M.; Lagojda, A.; Schaeffer, A. Quantitative  
533 Identification of Biogenic Nonextractable Pesticide Residues in Soil by <sup>14</sup>C-Analysis.

- 534 *Environ. Sci. Technol.* **2016**, *50* (12), 6415–6422.
- 535 (20) Trapp, S.; Brock, A. L.; Nowak, K.; Kästner, M. Prediction of the Formation of Biogenic  
536 Nonextractable Residues during Degradation of Environmental Chemicals from Biomass  
537 Yields. *Environ. Sci. Technol.* **2018**, *52* (2), 663–672.
- 538 (21) Brock, A. L.; Kästner, M.; Trapp, S. Microbial Growth Yield Estimates from Thermodynamics  
539 and Its Importance for Degradation of Pesticides and Formation of Biogenic Non-Extractable  
540 Residues. *SAR QSAR Environ. Res.* **2017**, *28* (8), 629–650.
- 541 (22) Benbrook, C. M. Trends in Glyphosate Herbicide Use in the United States and Globally.  
542 *Environ. Sci. Eur.* **2016**, *28* (1), 1–15.
- 543 (23) Barja, B. C.; Dos Santos Afonso, M. Aminomethylphosphonic Acid and Glyphosate  
544 Adsorption onto Goethite: A Comparative Study. *Environ. Sci. Technol.* **2005**, *39* (2), 585–  
545 592.
- 546 (24) Borggaard, O. K.; Gimsing, A. L. Fate of Glyphosate in Soil and the Possibility of Leaching  
547 to Ground and Surface Waters: A Review. *Pest Manag. Sci.* **2008**, *64* (4), 441–456.
- 548 (25) Simonsen, L.; Fomsgaard, I. S.; Svensmark, B.; Spliid, N. H. Fate and Availability of  
549 Glyphosate and AMPA in Agricultural Soil. *J. Environ. Sci. Health. B.* **2008**, *43* (5), 365–375.
- 550 (26) Al-Rajab, A. J.; Amellal, S.; Schiavon, M. Sorption and Leaching of <sup>14</sup>C-Glyphosate in  
551 Agricultural Soils. *Agron. Sustain. Dev.* **2008**, *28* (3), 419–428.
- 552 (27) Bento, C. P. M.; Yang, X.; Gort, G.; Xue, S.; van Dam, R.; Zomer, P.; Mol, H. G. J.; Ritsema,  
553 C. J.; Geissen, V. Persistence of Glyphosate and Aminomethylphosphonic Acid in Loess  
554 Soil under Different Combinations of Temperature, Soil Moisture and Light/Darkness. *Sci.*  
555 *Total Environ.* **2016**, *572*, 301–311.
- 556 (28) Nguyen, D. B.; Rose, M. T.; Rose, T. J.; Morris, S. G.; van Zwieten, L. Impact of Glyphosate  
557 on Soil Microbial Biomass and Respiration: A Meta-Analysis. *Soil Biol. Biochem.* **2016**, *92*,  
558 50–57.
- 559 (29) Grandcoin, A.; Piel, S.; Baures, E. AminoMethylPhosphonic Acid (AMPA) in Natural Waters:  
560 Its Sources, Behavior and Environmental Fate. *Water Res.* **2017**, *117*, 187–197.
- 561 (30) Pipke, R.; Amrhein, N.; Jacob, G. S.; Schaefer, J.; Kishore, G. M. Metabolism of Glyphosate  
562 in an *Arthrobacter*-Sp GIp-1. *Eur. J. Biochem.* **1987**, *165*, 267–273.
- 563 (31) Pipke, R.; Amrhein, N. Degradation of the Phosphonate Herbicide Glyphosate By  
564 *Arthrobacter-Atrocyaneus* Atcc-13752. *Appl. Environ. Microbiol.* **1988**, *54* (5), 1293–1296.
- 565 (32) Fitzgibbon, J.; Braymer, H. D. Phosphate Starvation Induces Uptake of Glyphosate by  
566 *Pseudomonas* Sp. Strain PG2982. *Appl. Environ. Microbiol.* **1988**, *54* (7), 1886–1888.
- 567 (33) McAuliffe, K. S.; Hallas, L. E.; Kulpa, C. F. Glyphosate Degradation by *Agrobacterium*  
568 *Radiobacter* Isolated from Activated Sludge. *J. Ind. Microbiol.* **1990**, *6* (3), 219–221.
- 569 (34) Klimek, M.; Lejczak, B.; Kafarski, P.; Forlani, G. Metabolism of the Phosphonate Herbicide  
570 Glyphosate by a Non-Nitrate-Utilizing Strain of *Penicillium Chrysogenum*. *Pest Manag. Sci.*  
571 **2001**, *57* (9), 815–821.
- 572 (35) Sviridov, A. V.; Shushkova, T. V.; Ermakova, I. T.; Ivanova, E. V.; Epiktetov, D. O.;  
573 Leontievsky, A. A. Microbial Degradation of Glyphosate Herbicides (Review). *Appl.*  
574 *Biochem. Microbiol.* **2015**, *51* (2), 188–195.
- 575 (36) Sviridov, A. V.; Shushkova, T. V.; Zelenkova, N. F.; Vinokurova, N. G.; Morgunov, I. G.;  
576 Ermakova, I. T.; Leontievsky, A. A. Distribution of Glyphosate and Methylphosphonate  
577 Catabolism Systems in Soil Bacteria *Ochrobactrum Anthropi* and *Achromobacter* Sp. *Appl.*  
578 *Microbiol. Biotechnol.* **2012**, *93* (2), 787–796.
- 579 (37) Hove-Jensen, B.; Zechel, D. L.; Jochimsen, B. Utilization of Glyphosate as Phosphate  
580 Source: Biochemistry and Genetics of Bacterial Carbon-Phosphorus Lyase. *Microbiol. Mol.*  
581 *Biol. Rev.* **2014**, *78* (1), 176–197.
- 582 (38) Wang, S.; Seiwert, B.; Kästner, M.; Miltner, A.; Schäffer, A.; Reemtsma, T.; Yang, Q.;  
583 Nowak, K. M. (Bio)Degradation of Glyphosate in Water-Sediment Microcosms - A Stable  
584 Isotope Co-Labeling Approach. *Water Res.* **2016**, *99*, 91–100.
- 585 (39) Zhan, H.; Feng, Y.; Fan, X.; Chen, S. Recent Advances in Glyphosate Biodegradation  
586 Glyphosate. **2018**.



- 587 (40) Li, H.; Wallace, A. F.; Sun, M.; Reardon, P. N.; Jaisi, D. P. Degradation of Glyphosate by  
588 Mn-oxide May Bypass Sarcosine and Form Glycine Directly after C–N Bond Cleavage.  
589 *Environ. Sci. Technol.* **2018**, acs.est.7b03692.
- 590 (41) Aparicio, V. C.; De Gerónimo, E.; Marino, D.; Primost, J.; Carriquiriborde, P.; Costa, J. L.  
591 Environmental Fate of Glyphosate and Aminomethylphosphonic Acid in Surface Waters and  
592 Soil of Agricultural Basins. *Chemosphere* **2013**, 93 (9), 1866–1873.
- 593 (42) Huntscha, S.; Stravs, M. A.; Bühlmann, A.; Ahrens, C. H.; Frey, J. E.; Pomati, F.; Hollender,  
594 J.; Buerge, I. J.; Balmer, M. E.; Poiger, T. Seasonal Dynamics of Glyphosate and AMPA in  
595 Lake Greifensee: Rapid Microbial Degradation in the Epilimnion During Summer. *Environ.*  
596 *Sci. Technol.* **2018**, acs.est.8b00314.
- 597 (43) Silva, V.; Montanarella, L.; Jones, A.; Fernández-Ugalde, O.; Mol, H. G. J.; Ritsema, C. J.;  
598 Geissen, V. Distribution of Glyphosate and Aminomethylphosphonic Acid (AMPA) in  
599 Agricultural Topsoils of the European Union. *Sci. Total Environ.* **2018**, 621, 1352–1359.
- 600 (44) VanBriesen, J. M.; Rittmann, B. E. Mathematical Description of Microbiological Reactions  
601 Involving Intermediates (Vol 67, Pg 35, 1999). *Biotechnol. Bioeng.* **2000**, 68 (6), 705.
- 602 (45) Flamholz, A.; Noor, E.; Bar-Even, A.; Milo, R. EQUilibrator - The Biochemical  
603 Thermodynamics Calculator. *Nucleic Acids Res.* **2012**, 40 (D1), 770–775.
- 604 (46) Thauer, R. K.; Jungermann, K.; Decker, K. Energy Conservation in Chemotrophic Anaerobic  
605 Bacteria. *Bacteriol. Rev.* **1977**, 41 (1), 100–180.
- 606 (47) Diekert, G. Grundmechanismen Des Stoffwechsels Und Der Energiegewinnung. In  
607 *Umweltbiotechnologie*; Ottow, J. C. G., Bidlingmaier, W., Eds.; Fischer Verlag: Stuttgart,  
608 Germany, 1997; pp 1–38.
- 609 (48) Christensen, D. R.; McCarty, P. L. Multi-Process Biological Treatment Model. *J. (Water*  
610 *Pollut. Control Fed.* **1975**, 47 (11), 2652–2664.
- 611 (49) LaRowe, D. E.; Van Cappellen, P. Degradation of Natural Organic Matter: A  
612 Thermodynamic Analysis. *Geochim. Cosmochim. Acta* **2011**, 75 (8), 2030–2042.
- 613 (50) FOCUS. Guidance Document on Estimating Persistence and Degradation Kinetics from  
614 Environmental Fate Studies on Pesticides in EU Registration. *Report of the FOCUS Work*  
615 *Group on Degradation Kinetics, EC Sanco/10058/2005*. 2006, pp 1–434.
- 616 (51) Vrugt, J. A. Markov Chain Monte Carlo Simulation Using the DREAM Software Package:  
617 Theory, Concepts, and MATLAB Implementation. *Environ. Model. Softw.* **2016**, 75, 273–  
618 316.
- 619 (52) Tchobanoglous, G.; Burton, F.; Stensel, H. *Wastewater Engineering - Treatment and Reuse*,  
620 4th ed.; McGraw-Hill, New York, US., 2003.
- 621 (53) Adam, I. K.; Rein, A.; Miltner, A.; da Costa, F. A.; Trapp, S.; Kaestner, M. Experimental  
622 Results and Integrated Modelling of Bacterial Growth on Insoluble Hydrophobic Substrate  
623 (Phenanthrene). *Env. Sci Technol* **2014**, 48, 8717–8726.
- 624 (54) Rein, A.; Adam, I. K. U.; Miltner, A.; Brumme, K.; Kästner, M.; Trapp, S. Impact of Bacterial  
625 Activity on Turnover of Insoluble Hydrophobic Substrates (Phenanthrene and Pyrene)-Model  
626 Simulations for Prediction of Bioremediation Success. *J. Hazard. Mater.* **2016**, 306, 105–  
627 114.
- 628 (55) Wang, S.; Miltner, A.; Nowak, K. M. Identification of Degradation Routes of Metamitron in  
629 Soil Microcosms Using <sup>13</sup>C-Isotope Labeling. *Environ. Pollut.* **2017**, 220, 927–935.
- 630 (56) Wang, S.; Miltner, A.; Kästner, M.; Schäffer, A.; Nowak, K. M. Transformation of Metamitron  
631 in Water-Sediment Systems\_ Detailed Insight into the Biodegradation Processes. *Sci. Total*  
632 *Environ.* **2017**, 578, 100–108.
- 633 (57) Madigan, M. T., Martinko, J. M., Bender, K. S., Buckley, D. H., & Stahl, D. A. *Brock Biology*  
634 *of Microorganisms*, 14th ed.; Pearson Inc.: Boston, USA, 2014.
- 635 (58) Frutiger, J.; Marcarie, C.; Abildskov, J.; Sin, G. A Comprehensive Methodology for  
636 Development, Parameter Estimation, and Uncertainty Analysis of Group Contribution Based  
637 Property Models-An Application to the Heat of Combustion. *J. Chem. Eng. Data* **2016**, 61  
638 (1), 602–613.
- 639 (59) Pipke, R.; Amrhein, N. Isolation and Characterization of a Mutant of *Arthrobacter* Sp. Strain

- 640 GLP-1 Which Utilizes the Herbicide Glyphosate as Its Sole Source of Phosphorus and  
641 Nitrogen. *Appl. Environ. Microbiol.* **1988**, *54* (11), 2868–2870.
- 642 (60) la Cecilia, D.; Maggi, F. Analysis of Glyphosate Degradation in a Soil Microcosm. *Environ.*  
643 *Pollut.* **2018**, *233*, 201–207.
- 644 (61) Button, D. K. Kinetics of Nutrient-Limited Transport and Microbial Growth. *Microbiol. Rev.*  
645 **1985**, *49* (3), 270–297.
- 646 (62) la Cecilia, D.; Tang, F. H. M.; Coleman, N. V.; Conoley, C.; Vervoort, R. W.; Maggi, F.  
647 Glyphosate Dispersion, Degradation, and Aquifer Contamination in Vineyards and Wheat  
648 Fields in the Po Valley, Italy. *Water Res.* **2018**, *146*, 37–54.
- 649 (63) Muskus, A. M.; Krauss, M.; Miltner, A.; Hamer, U.; Nowak, K. M. Effect of Temperature, PH  
650 and Total Organic Carbon Variations on Microbial Turnover of <sup>13</sup>C<sup>15</sup>N-Glyphosate in  
651 Agricultural Soil. *Sci. Total Environ.* **2019**, *658*, 697–707.
- 652 (64) Kästner, M.; Nowak, K. M.; Miltner, A.; Schäffer, A. (Multiple) Isotope Probing Approaches to  
653 Trace the Fate of Environmental Chemicals and the Formation of Non-Extractable ‘Bound’  
654 Residues. *Curr. Opin. Biotechnol.* **2016**, *41*, 73–82.
- 655 (65) Fraser, F. C.; Corstanje, R.; Deeks, L. K.; Harris, J. A.; Pawlett, M.; Todman, L. C.;  
656 Whitmore, A. P.; Ritz, K. On the Origin of Carbon Dioxide Released from Rewetted Soils.  
657 *Soil Biol. Biochem.* **2016**, *101*, 1–5.
- 658 (66) Gimsing, A. L.; Borggaard, O. K.; Sestoft, P. Modeling the Kinetics of the Competitive  
659 Adsorption and Desorption of Glyphosate and Phosphate on Goethite and Gibbsite and in  
660 Soils. *Environ. Sci. Technol.* **2004**, *38* (6), 1718–1722.
- 661

